

Synthesis Cytotoxic Effect and DFT Investigation of some Benzoyl Thiourea Compounds

Ahmed Hamed Al-Yaqoubi and Rafid H. Al-Asadi

Department of Chemistry, College of Education for Pure Sciences, University of Basrah, 61004 Basrah, Iraq
 ahmedhamedk98@gmail.com, rafid.abdalabass@uobasrah.edu.iq

Keywords: Thiourea Benzamide, LUMO, HOMO, DFT, Breast Cancer.

Abstract: Benzoyl thiourea derivatives have garnered significant interest due to their diverse biological and pharmacological properties. A series of benzoyl thiourea derivatives (L1–L5) were synthesized using 4-nitrobenzoyl chloride and 4-methoxybenzoyl chloride as starting acylating agents, reacting with various amines, including 3,4-dimethylaniline, benzene-1,2-diamine, and ethane-1,2-diamine. The chemical structures of the synthesized compounds were confirmed through various spectroscopic techniques, including electron ionization mass spectrometry (EI-MS), Fourier-transform infrared spectroscopy (FT-IR), ^1H and ^{13}C nuclear magnetic resonance (NMR) spectroscopy, as well as melting point analysis. To support and rationalize the experimental findings, a comprehensive theoretical investigation was performed using Density Functional Theory (DFT) with the B3LYP functional and 6-31G++(d,p) basis set. The computational study involved the determination of frontier molecular orbital energies (HOMO and LUMO), Mulliken atomic charges, and selected structural parameters. Furthermore, the analysis identified key donor atoms in each molecule, providing insights into their electronic behavior. The in vitro cytotoxic potential of the synthesized compounds (L1–L5) was assessed against MCF-7 human breast cancer cell lines using the MTT assay. The results revealed that the compounds exhibited low cytotoxic efficacy under the tested conditions.

1 INTRODUCTION

Thioureas and urea are exceptional chemicals in organic chemistry [1]. Their properties allow them to serve as versatile building blocks in the development of various compounds, including agricultural chemicals and dyes [2]. Thioureas have seen promise in materials science, especially in the production of medical and pharmaceutical chemicals and biological [3]. Many different chemicals can be made from thiourea because it has two active main amino groups. It can also be used to make other chemicals sectors of the pharmaceutical business, owing to its biological properties. It can fight many types of cancer if found early, so these actions include both antiparasitic and anticancer effects [4].

Thiourea derivatives demonstrate notable efficacy in the treatment of breast, prostate, and lung cancer. They also demonstrate anti-tuberculosis, antibacterial, and analgesic effects. Researchers recognize benzoyl thiourea derivatives for their extensive antioxidant, antifungal, antibacterial, antitumor, anti-inflammatory, and antidiabetic properties [5], [6]. Thiourea consists of three distinct

functional groups: imino, thiol and amine. Because there are two NH_2 groups on either side of the $\text{C}=\text{S}$ bond, there are more possible derivatives of Thiourea [7], [8]. They have two strong donating groups, called carbonyl and thiourea, these groups provide both hard and soft donor sites for metal coordination through nitrogen (N), oxygen (O), and sulfur (S) atoms [9]. Carbonyl thiourea can bind anions well because it has two imine groups ($-\text{NH}$) on both the urea and thiourea parts [10]. thiourea to replicate the natural binding mechanisms present in live cells, and thiocarbonyl groups ($\text{C}=\text{S}$) in carbonyl thiourea may make the product more acidic, which makes it easier for anions to bind to a similar compound that has a carbonyl group ($\text{C}=\text{O}$) [11]. Compounds with thiocarbonyl groups are stable because hydrogen bonds form inside the molecules and molecules interact with each other [12], sulfur (S), nitrogen (N), and oxygen (O) atoms that act as both soft and hard bases, therefore it's very important for coordinating with metal ions [13], [14]. The aim of the study is to prepare five compounds of benzoyl thiourea derivatives (L1-L5) and evaluate the biological activity of the prepared compounds as anti-breast cancer cells and conduct a

theoretical study of the prepared compounds using computational chemistry to analyze some electronic properties.

2 MANUSCRIPT PREPARATION

4-methoxy benzoyl chloride, 4-nitrobenzoyl chloride, Potassium thiocyanate, benzene-1,2-diamine, 3,4-dimethyl aniline, ethane-1,2-diamine, acetone, ethanol, methanol, ethyl acetate, diethyl ether, chloroform and hexane were purchased from Merck and Sigma-Aldrich. The purity level of the compounds was very high (around 97–99%).

2.1 Instrumentation

Melting Point was measure by equipment from Thermo Scientific. Using the KBr method, infrared spectra were collected in the 400–4000 cm^{-1} range using FT-IR 84005-SHIMADZU device. The compounds' ^1H -NMR and ^{13}C -NMR spectra were captured using deuterated DMSO solvents on a Bruker 400MHz spectrometer. The EI-MS spectra of the compounds was analyzed using Agilent Technologies 5975C spectrometer .

2.2 Synthesis of the Compounds (L1-L5).

The preparation methods were followed according to the literature with some modifications [15], [16].

2.2.1 3-(3,4-Dimethylphenyl)-1-(4-Nitrobenzoyl) Thiourea L1

A solution (10 mmol) containing 1.85g of 4-nitro benzoyl chloride in 15 mL of acetone was added progressively to a solution containing 0.97 g (10 mmol) of potassium thiocyanate in 10 mL of acetone. The mixture was refluxed for 1 h with stirring, and the product was filtered, then added while hot to a solution that was made from 1.21g (10 mmol) of 3,4-dimethyl aniline in 20 mL acetone. The mixture was refluxed with a stirrer for 4 h, and followed by thin layer chromatographic (TLC) analysis (ethyl acetate: hexane, 3:7). The yield was cooled, filtered, dried, and recrystallized using hot absolute ethanol. The product was a light yellow solid. Yield= 44%, m.p: 187-189°C .IR data, ν_{max} , cm^{-1} : 3217 (NH stretch), 3055 (CH-Ar), 1664 (C=O amide), 1590(C=C) and 1522 (NO_2), 1140 (C=S). ^1H NMR(400MHz,DMSO- d_6), δ ppm:12.35(s,1H,H4),11.93(s,1H,H3),8.34(d,2H,H1),8.17(d,2H,H2)

,7.46(d,1H,H9),7.41(s,1H,H5),7.18(d, 1H, H8), 2.23 (s,6H,H6). ^{13}C NMR(100MHz,DMSO- d_6), δ ppm178.93(C9),167.25(C7),150.22(C2),138.54(C11),137.11(C5),135.99(C12),135.06(16),130.72(C1+C3),130.01(C13),125.60(C14),123.79(C4+C6),122.02(C15),19.90(C18),19.44(C17),(EI-MS,m/z (%)):329.1[M+, 13].

2.2.2 1-(3,4-Dimethylphenyl)-3-(4-Methoxybenzoyl)Thiourea L 2

A similar procedure was used as in compound L1 except instead of 4-nitro benzoyl chloride, 1.35 ml of (10 mmol) was employe 4-methoxy benzoyl chloride. The product was a white solid crystal, Yield=64%, m.p:144-164°C. IR data, ν_{max} , cm^{-1} : 3275 (NH stretch), 2965(CH-Ar),1666(C=O amide),1587(C=C), and,1137(C=S). ^1H NMR(400 MHz, DMSO- d_6), δ ppm12.67 (s,1H, H5), 11.36 (s,1H, H4) ,8.03 (d, 2H, H2),7.44 (m, 2H, H8+H9), 7.43 (s,1H, H6) ,7.06(d, 2H, H1), 3.86(s, 3H, H3), 2.23(s,6H,H7), ^{13}C NMR(100MHz, DMSO- d_6), δ ppm:179.43(C9), 168.06 (C7),163.70(C2) ,137.06(C11),136.12(C5),134.86(C12),131.45(C1+C3),129.98(C16),125.63(C13),124.31(14),122.02(C15)114.27 (C6+C4)56.08 (C22)19.90 (C17)19.43 (C18), (EI- MS, m/z (%)):314.3 [M+, 26].

2.2.3 1-(4-Nitrobenzoyl)-3-[2-((4-Nitrophenyl) Formamido)Methanethioyl] Amino)Phenyl] Thiourea L 3

A solution (10 mmol) containing 1.85g of 4-nitro benzoyl chloride in 15 mL of acetone was added progressively to a solution containing 0.97 g (10 mmol) of potassium thiocyanate in 10 mL of acetone. The mixture was refluxed for 1 h with stirring, and the product was filtered, then added while hot to a solution that was made benzene-1,2-diamine containing 0.54g of (5mmol) in 20 mL acetone. The mixture was refluxed with a stirrer for 6 h, and followed by TLC analysis (ethyl acetate: hexane, 3:7). The yield was cooled, filtered, dried, and recrystallized using hot absolute ethanol. The product was a light yellow solid. Yield=33%, m.p: 198-200°C. IR data, ν_{max} , cm^{-1} :3362 and 3119 (NH stretch), 3061 (CH-Ar), 1661(C=O amide), 1596, (C=C), 1510 (NO_2), 1143(C=S). ^1H NMR (400MHz, DMSO- d_6), δ ppm:12.31(s, 2H, H3), 12.16(s, 2H, H4), 8.40(d, 4H, H6), 8.10(d, 4H, H5), 7.94(d, 2H, H2),7.44(d,2H,H1). ^{13}C NMR(100MHz,DMSO- d_6), δ ppm:180.61(C9+C27),167.35(C7+C25),150.32(C3+C21),138.36(C17+C18),133.86(C6+C24),130.70(C2+

C4+C20+C22),127.76(C13+C16),127.23(C14+C15), 123.87(C1+C5+C19+C23).

2.2.4 3-(4-Methoxybenzoyl)-1-[2-(((4-Methoxyphenyl)Formamido]Methanethioyl)Amino) Phenyl] Thiourea L 4

The same steps as in compound L3 were followed, but instead of 4-nitro benzoyl chloride, 1.35 ml of (10 mmol) 4-methoxy benzoyl chloride. The product was a white solid. Yield=20%, m.p 211-213°C. IR data, ν_{\max} , cm^{-1} : 3277 and 3207 (NH stretch), 2958 (aliphatic-CH), 1654 (C=O amide), 1598 (C=C), and 1149 (C=S). ^1H NMR (400 MHz, DMSO- d_6), δ ppm: 12.57 (s, 2H, H3), 11.56 (s, 2H, H4), 7.89 (d, 4H, H6), 7.39 (m, 4H, H1+H2), 7.04 (d, 4H, H5), 3.85 (s, 6H, H7), ^{13}C NMR (100 MHz, DMSO- d_6), δ ppm: 181.09 (C27+C9), 168.01 (C25+C7), 163.71 (C20+C3), 134.03 (C17+C18), 131.48 (C2+C4+C20+C22), 127.5 (C6+C24), 127.24 (C13+C16), 124.20 (C14+C15), 114.21 (C1+C5+C19+C23), 56.08 (C32+C34).

2.2.5 3-(4-Methoxybenzoyl)-1-[2-(((4-Methoxyphenyl)Formamido]Methanethioyl)Amino) Ethyl]Thiourea L 5

The same steps as in compound L3 were followed, but instead of 4-nitro benzoyl chloride, 1.35 ml of (10 mmol) 4-methoxy benzoyl chloride was used, and instead of benzene-1,2-diamine by 0.33 ml (5 mmol) of ethane-1,2-diamine. The product was a white solid. Yield=29%, m.p: 177-179 °C. IR data, ν_{\max} , cm^{-1} : 3243 and 3179 (NH stretch), 2940 (aliphatic CH), 1668 (C=O amide), 1606.29 (C=C) and 1166.72 (C=S). ^1H NMR (400 MHz, DMSO- d_6), δ ppm: 11.20 (s, 2H, H2), 11.04 (s, 2H, H3), 7.97 (d, 4H, H5), 7.04 (d, 4H, H4), 3.97 (d, 6H, H6), 3.84 (d, 4H, H1), ^{13}C NMR (100 MHz, DMSO- d_6), δ ppm: 181.49 (C4+C6), 167.51 (C8+C11), 163.53 (C15+C20), 131.29 (C14+C16+C19+C21), 124.41 (C9+C12), 114.19 (C13+C17+C18+C22), 56.03 (C28+C30), 43.79 (C1+C2).

2.3 Anti-Cancer Activity

Cell lines and culture. MDA-MB-231 (a human breast cancer cell line) was purchased from National Cell Bank of Iran (Pasteur Institute, Iran). Cells were grown in RPMI-1640 medium (Gibco) with 10% FBS (Gibco) supplemented with antibiotics (100 U/ml penicillin and 100 $\mu\text{g}/\text{ml}$ streptomycin), respectively. Cells were maintained at 37 °C under humidified air containing 5% CO_2 and were passaged using

trypsin/EDTA (Gibco) and phosphate-buffered saline (PBS) solution [15].

2.4 Computational Study

Geometry Optimization of the prepared compounds (L1-L5) was performed by configuring them using the semi-empirical method, then calculate employed by the DFT (density function method at the (B3LYP) level and using the basis set 6-31G++ (d,p) [17] using the Gaussian 09 program.

2.5 Results and Discussion

Production of the compounds (L1-L5) The reaction between Potassium thiocyanate and 4-nitrobenzoyl chloride and 4-methoxybenzoyl chloride at a 1:1 mole ratio produced benzoyl iso thiocyanate derivatives, as shown in Figure 1, while the reaction between the product with the 3,4-dimethylaniline at a 1:1 mole ratio resulted in thiourea benzamide derivative compounds L1 and L2, as presented in Figure 1. In addition, the reaction between the product with the benzene-1,2-diamine and ethane-1,2-diamine at a 2:1 mole ratio resulted in thiourea benzamide derivative compounds L3, L4 and L5, as presented in Figure 1 [16].

2.6 Characterization Methods

Figure 2 showed the ^1H NMR spectra of compounds, multiple signals at 7.01–8.40 ppm, which are associated with aromatic protons [18]. The presence of the amide group (-NH) was confirmed by a single peak observed at 11.93, 11.36, 12.16, 11.56 and 11.04 ppm for compounds (L1–L5), respectively [19], while the proton signal of the (-NH) group appeared as a singlet at 12.35, 12.67, 12.31, 12.57, and 11.20 ppm. The spectra of the compounds L2, L4 and L5 showed a single peak at 3.86, 3.85 and 3.84 ppm respectively, which could be attributed to the presence of (O-CH₃) protons in the final compounds. The spectra of the compounds L1 and L2 showed a single peak at 2.23 ppm, which could be attributed to the presence of (Ar-CH₃) protons in the final compounds. The spectra of the compound L5 showed a single peak at 3.97 ppm, which could be attributed to the presence of (Aliphatic -CH₂) protons.

^{13}C NMR spectra were observed at 178.93, 179.43, 180.61, 180.09 and 181.49 ppm, which correspond to the carbons of the C=S group in, compounds (L1-L5)

respectively (Fig. 3). However, the signals at 167.25, 168.06, 167.35, 168.01 and 167.51 ppm were assigned to the carbon of the carbonyl group (C=O) [20], [18] in compounds (L1-L5) respectively. The aromatic carbons were manifested in the range of 114.19 -163.71 ppm. However, the corresponding peak related to the(O-CH₃) aliphatic carbons appeared at 56.08 ,56.08 and 56.03 ppm in compounds L2, L4 and L5 respectively, and the corresponding peak related to the(CH₂) aliphatic carbons appeared at 43.79 ppm in the. compounds L5. the corresponding peak related to the (Ar-CH₃) appeared at the range (19.43 and 19.90)ppm in compounds L1 and L2 respectively.

Figure 4 presents the infrared spectra of the synthesized compounds (L1–L5), with band assignments based on literature [20], [21]. The spectra exhibited bands of varying intensities (weak, medium, and strong). Weak peaks at 3217, 3275 (L1), 3277, 3207 (L3), and 3243–3179 cm⁻¹ (L2, L4, L5) were assigned to N-H stretching vibrations. Aromatic C-H stretching (symmetric/asymmetric) appeared at 3055 cm⁻¹ (L1) and 3061 cm⁻¹ (L3). Aliphatic C-H stretches were observed at 2965, 2901 cm⁻¹ (L2), 2958 cm⁻¹ (L4), and 2940 cm⁻¹ (L5), displaying medium-to-strong intensity.

Weak C=O stretches were detected for all compounds (L1–L5), while aromatic C=C vibrations

showed average intensity at 1590 cm⁻¹ (L1), 1587 cm⁻¹ (L2), 1596 cm⁻¹ (L3), 1598 cm⁻¹ (L4), and 1606 cm⁻¹ (L5). NO₂ stretches produced strong bands at 1522–1331 cm⁻¹ (L1) and 1510–1329 cm⁻¹ (L3). The C=S group resonated strongly at 1140 cm⁻¹ (L1), 1137 cm⁻¹ (L2), 1143 cm⁻¹ (L3), 1149 cm⁻¹ (L4), and 1166 cm⁻¹ (L5).

In EI-MS spectra, fragments at m/z 150, 135, 150, 135, 135 corresponded to ions (C₇H₄NO₃)⁺ (L1, L3) and (C₈H₇O₂)⁺ (L2, L4, L5). Shared base ions reflect structural similarities between L1/L3 and L2/L4/L5. Fragment diversity confirms successful synthesis [22].

Figure 5 presents the EI-MS spectra of compounds L1–L5. Compound L1 showed a molecular ion peak at m/z = 329.1 ([C₁₆H₁₅O₃N₃S]⁺) with a relative abundance of 13%. Compound L5 showed a peak at m/z = 314.40 ([C₁₇H₁₈O₂N₂S]⁺). In relative abundance (26%) compound L2, and The molecular ion peak of the compounds L3, L4, L5 appeared with a very low relative abundance ranging between (3-5)%, The reason is that their molecular ions are unstable and dissociate easily due to their large molar masses. The bass peaks ion of the prepared compounds (L1- L5) appeared respectively in relative abundance 100.

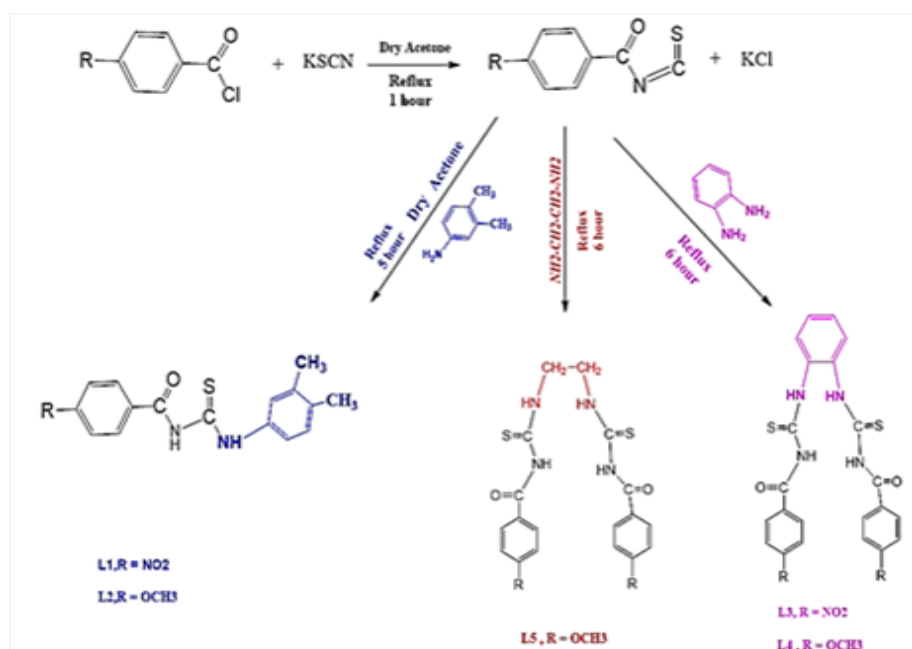
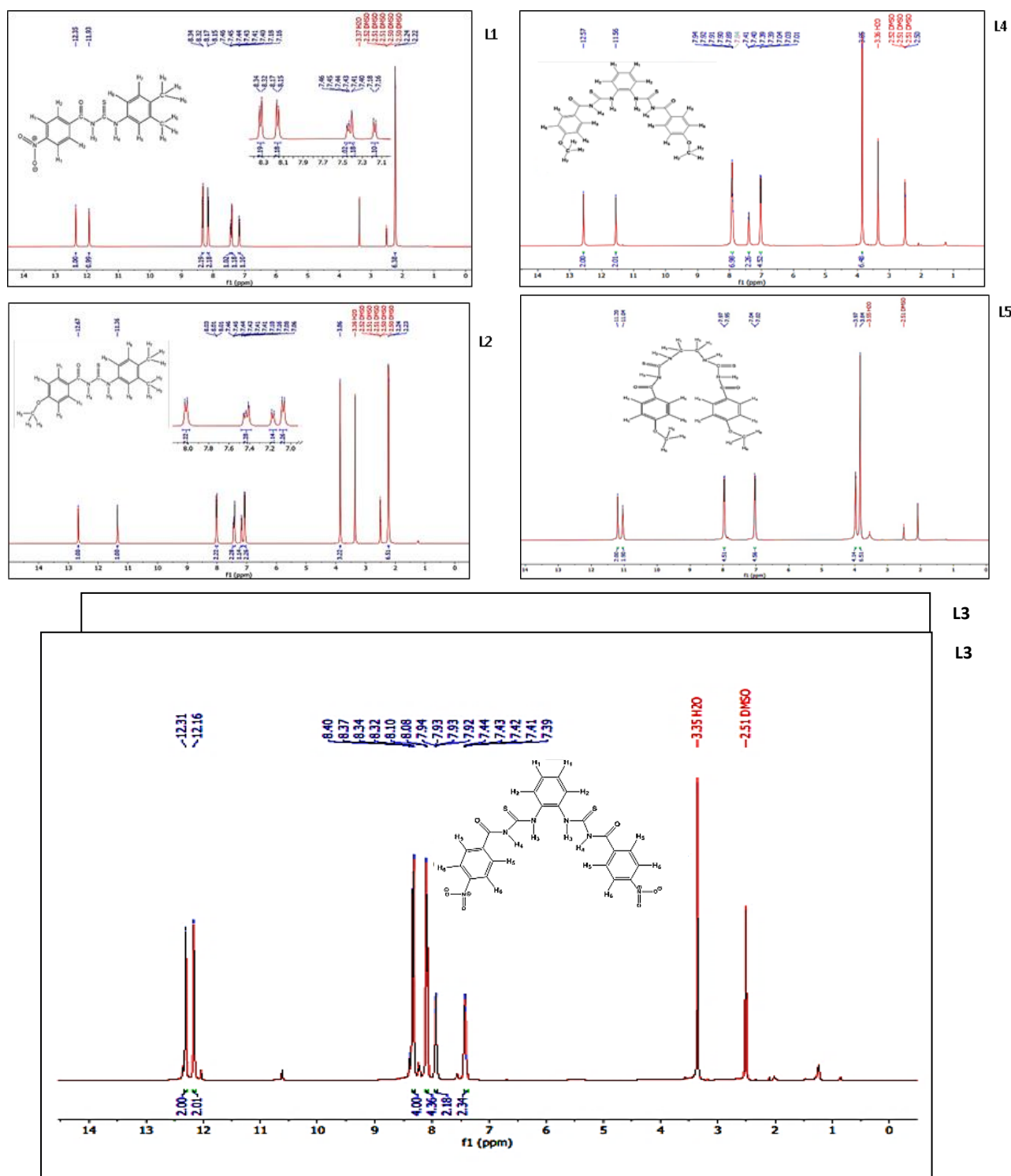
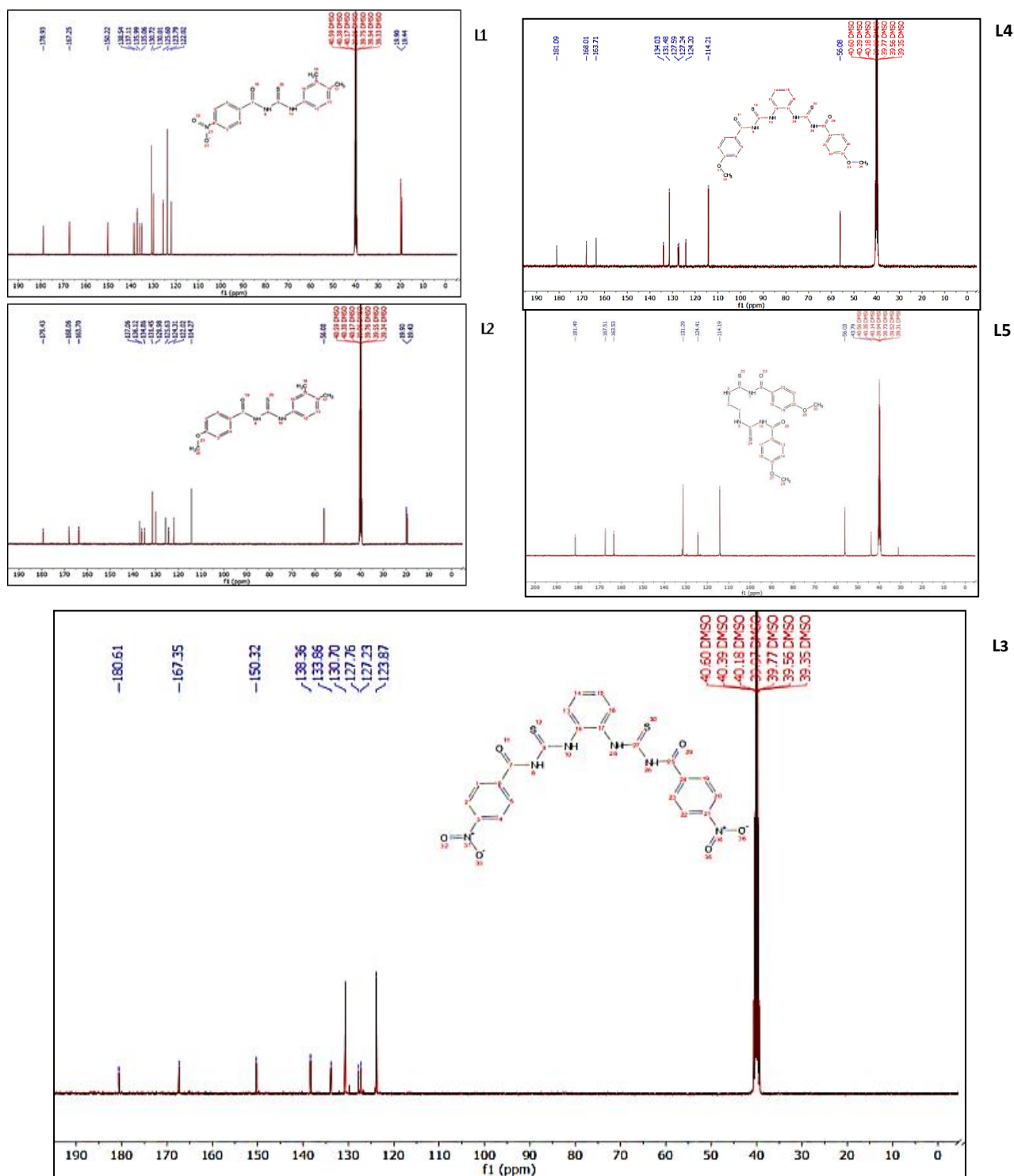


Figure 1: Preparation pathway to compounds (L1 – L5).





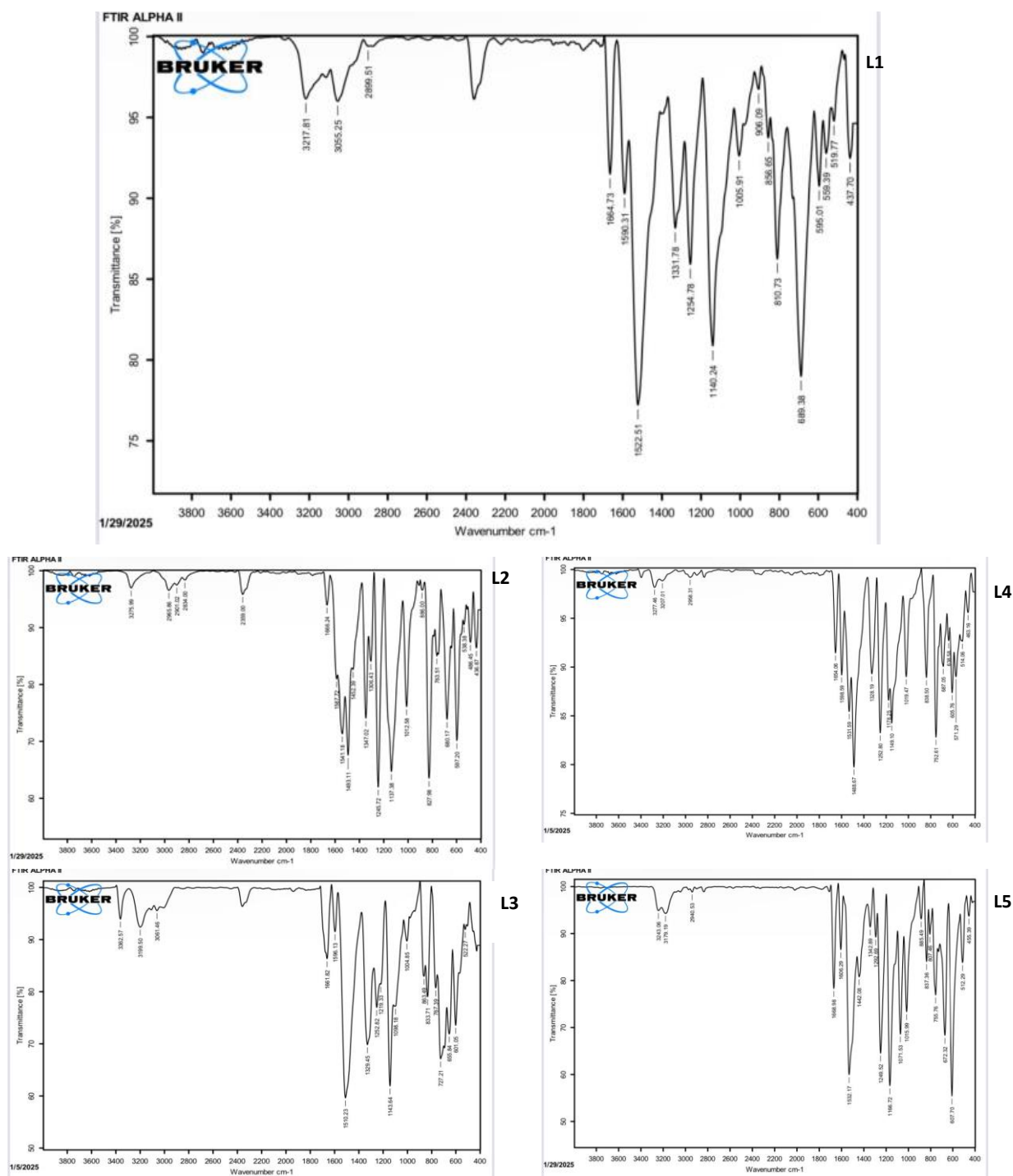


Figure 4: FT-IR spectra of compounds (L1-L5).

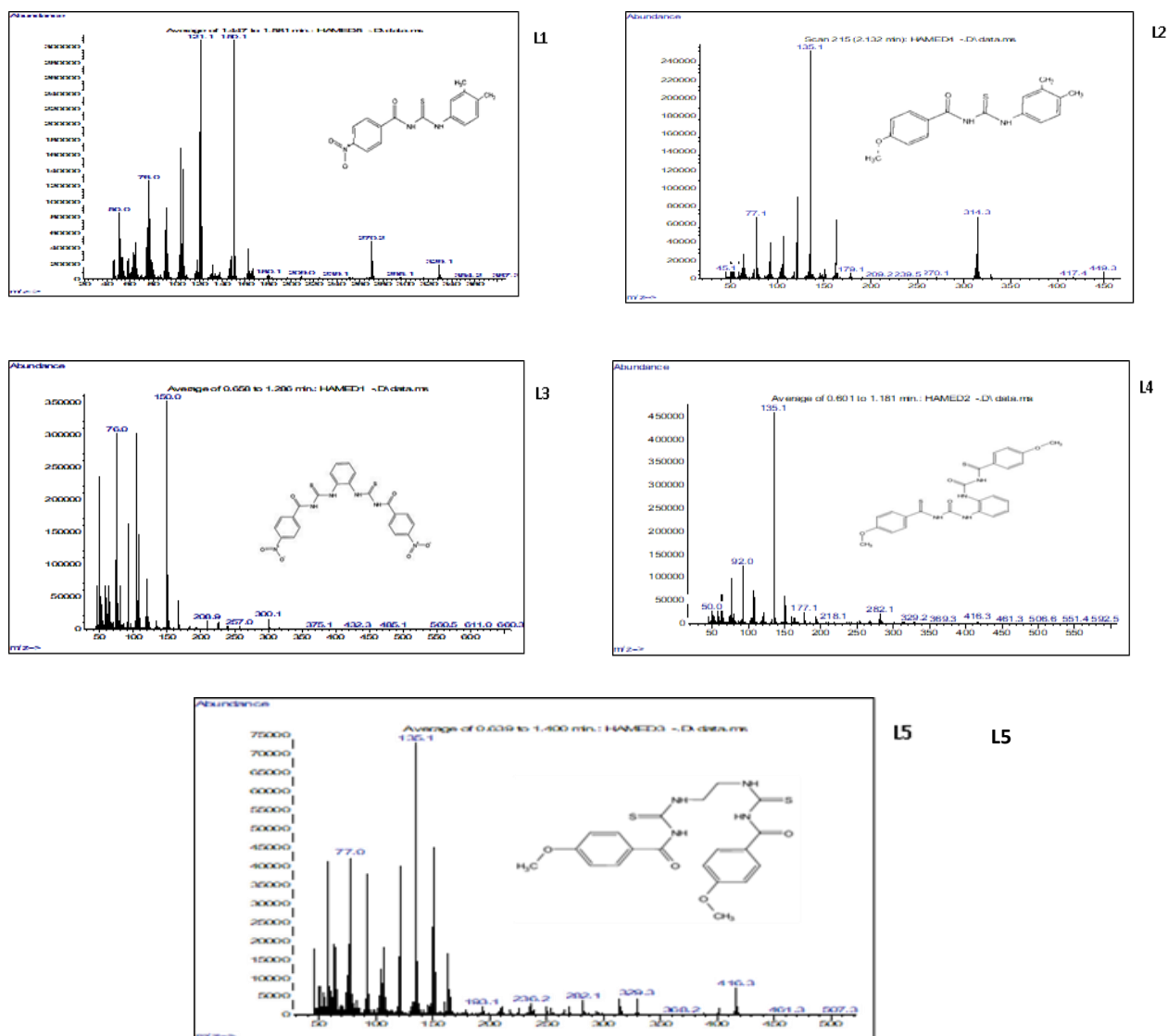


Figure 5: EI-MS spectra of compounds (L1-L5).

2.6 Anticancer Efficacy Study

The toxicity of compounds L1, L2, L3, L4, and L5 against type MCF-7 breast cancer cells was studied *in vitro*. The study was conducted using five different concentrations of (7.4, 22.2, 66.6, 200 and 600) micrograms per milliliter ($\mu\text{g/ml}$) for each compound, respectively. The inhibitory efficacy was calculated at each concentration, along with the IC_{50} values. Low efficacy in killing cancer cells was demonstrated [15], as is evident from the values shown in Table 1.

2.7 Structural Parameters of the Molecular Structure

The important structural parameters of the optimized geometries were summarized, such as calculating the bond lengths and the triple and quadruple angles of the selected benzoylthiourea derivatives studied (L1-L5). It was found that there was no noticeable change in the bond lengths despite the difference in the substitutes. As we note in Table 2, there is a convergence between the values of the bond lengths, triple and quadruple angles of the studied compounds with the practical values. This confirms that this function is correct and suitable for this type of compounds (Fig. 6).

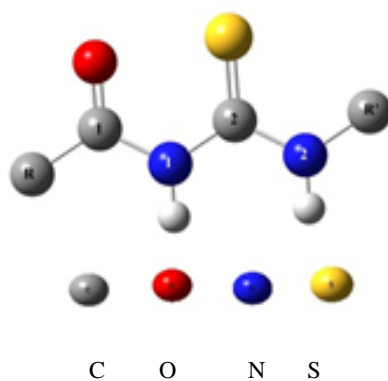


Figure 6: Structural parameters of the molecular structure.

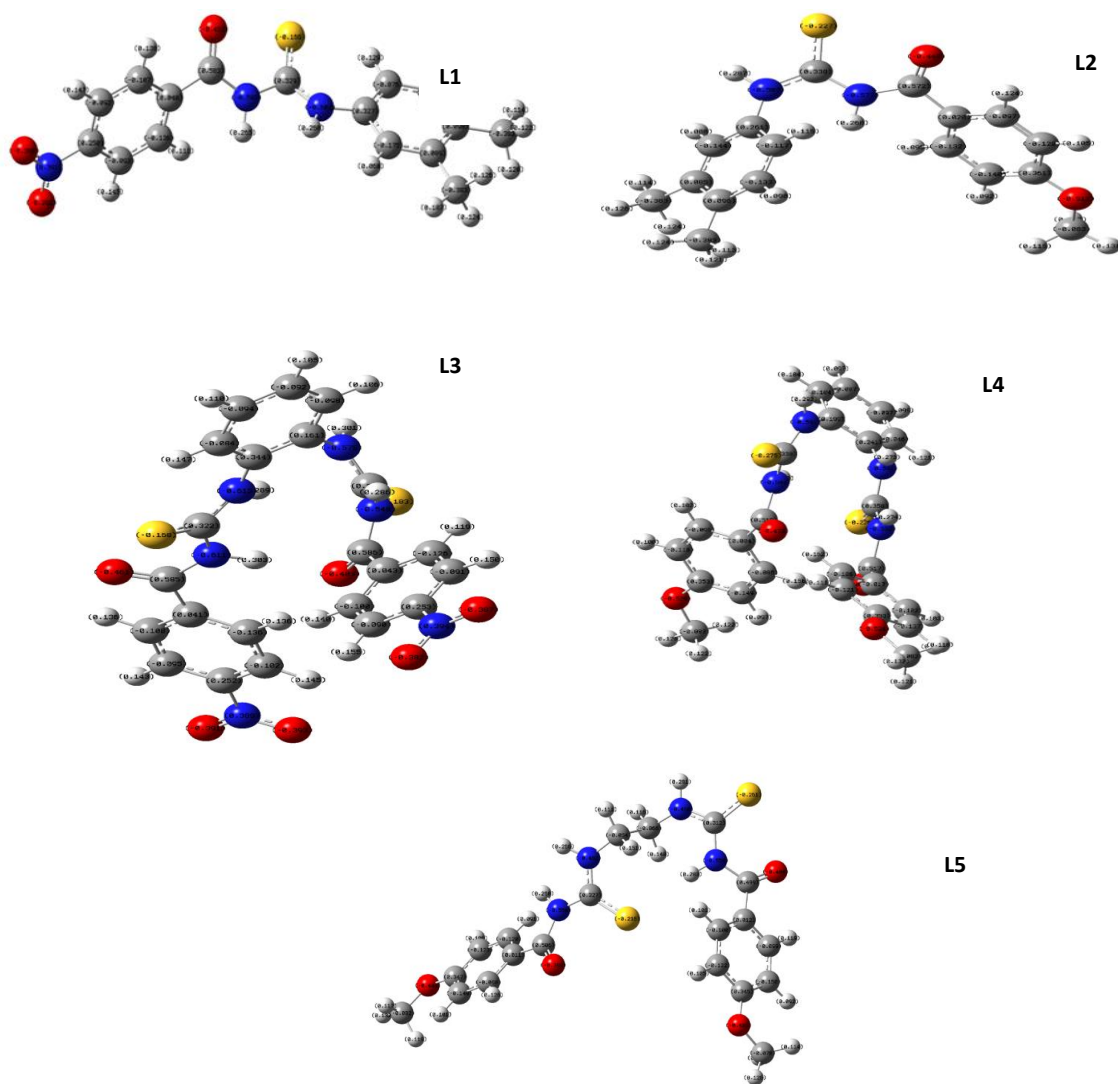


Figure 7: Mulliken charge indicator on atoms of compounds (L1-L5).

Table 1: Inhibition potential of studied compounds against MCF-7 cell line and IC₅₀ values.

Comp.No	7.4	22.22	66.66	200	600	IC ₅₀ (μg/mL)
L1	2.65	10.15	22.12	38.71	55.08	491.61
L2	8.94	16.52	26.74	34.55	41.52	1662.56
L3	5.83	12.65	22.12	42.12	64.32	312.13
L4	4.92	9.62	23.48	28.48	50.15	972.40
L5	7.5	10.83	21.97	38.79	49.92	702.07

Table 2: The bond lengths, triple angles, and quadruple angles of the studied compounds were calculated using the method by the DFT/B3LYP 6-31G(d,p) compounds (L1-L5).

Bond Lengths (Å)	L1	L2	L3	L4	L5	Experimental values *
C _R -C1	1.50721	1.49014	1.50654	1.49440	1.49329	1.506
C1=O	1.21466	1.19951	1.21581	1.21767	1.21367	1.221
C1-N1	1.39392	1.44943	1.39695	1.40702	1.41394	1.391
N1-C2	1.42111	1.39927	1.40845	1.40003	1.39319	1.376
C2=S	1.65365	1.65897	1.65389	1.65728	1.66785	1.663
C2-N2	1.36497	1.38529	1.37697	1.38106	1.36482	1.376
N2-C _R '	1.41556	1.43994	1.40631	1.40288	1.45730	1.338
Triple angles (°)	L1	L2	L3	L4	L5	Experimental values *
C _R -C1-O	121.68369	126.73713	121.53657	122.31454	123.07146	121.74
O-C1-N1	123.95781	121.85704	123.08154	122.14930	122.95462	122.12
C1-N1-C2	126.69775	122.60050	125.54131	125.77605	128.29953	129.09
N1-C2-S	122.21285	122.18932	123.48392	123.78686	124.62692	118.26
S-C2-N2	128.48475	118.15765	127.23150	126.90540	123.65244	127.94
Quadruple angles (°)	L1	L2	L3	L4	L5	
C _R -C1-N1-C2	167.66041	-171.11323	-167.42515	-167.95513	-168.98623	
O-C1-N1-C2	-14.63761	10.49827	15.01441	14.59979	13.42432	
C1-N1-C2-N2	138.97839	-172.28886	-140.82613	-142.09091	-154.87123	
C1-N1-C2-S	-43.38889	10.11958	-165.52039	39.99027	28.02735	
N1-C2-N2-C _R '	168.65784	6.62085	15.0758	-164.84228	-178.51631	
S-C2-N2-C _R '	-8.78332	-175.69095	11.49652	12.99456	-1.38162	

*Ref: [17]

Table 3: Calculated values of total energy and LUMO-HOMO energy gap for the studied compounds(L1-L5).

No.	Total energy (eV)	Dipole moment (Debye)	HOMO energy (eV)	LUMO energy (eV)	ΔE (eV)
L1	-31934.4188	6.9287	-6.211401	-4.896844	1.31455
L2	-29892.2335	9.8211	-6.218438	-4.388818	1.82962
L3	-55026.5903	10.1441	- 6.201413	- 4.929759	1.27165
L4	-50941.9959	6.1638	- 5.92697	- 4.163634	1.76333
L5	-47481.0062	13.3499	- 6.135356	- 4.220838	1.91451

Table 4: HOMO and LUMO orbital shapes of the prepared compounds(L1-L5).

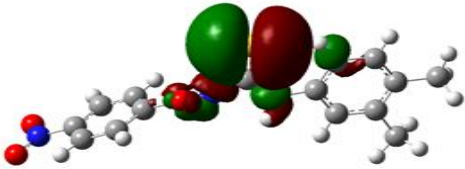
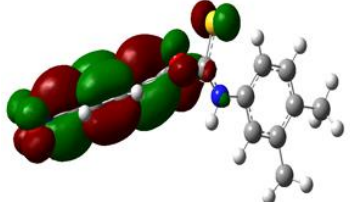
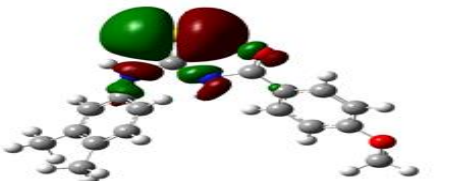
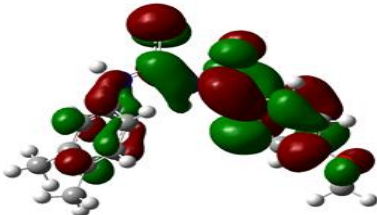
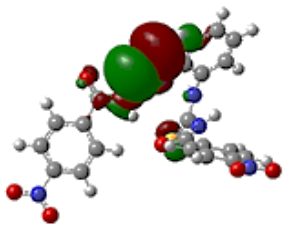
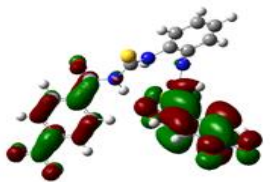
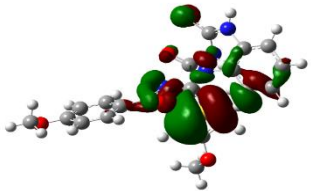
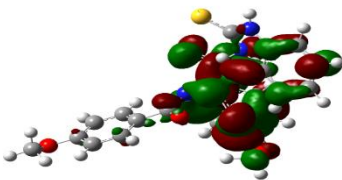
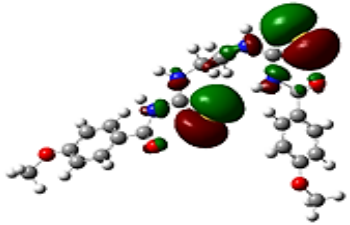
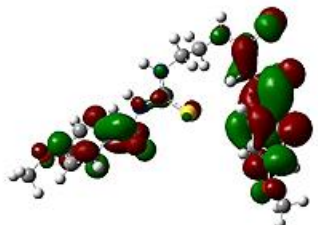
	HOMO	LUMO
L1		
L2		
L3		
L4		
L5		

Table 5: Mulliken charge values of prepared ligands calculated by DFT/B3LYP method 6-31G++(d,p).

Atoms	L1	L2	L3	L4	L5
O	-0.452	-0.449	-0.461	-0.413	-0.399
N1	-0.593	-0.577	-0.611	-0.552	-0.554
S	-0.166	-0.227	-0.168	-0.226	-0.216
N2	-0.602	-0.587	-0.613	-0.591	-0.482

2.8 Calculating of Energies

Molecular orbitals and their properties are very useful for physicists and chemists in particular, the highest occupied molecular orbital (HOMO) and the lowest empty molecular orbital (LUMO) and the energy gap between them reflect the chemical activity of the molecule. The energy values of the orbitals $\Delta E_{(LUMO-HOMO)}$, Highest Occupied Molecular Orbital (HOMO), Lowest Unoccupied Molecular Orbital (LUMO). The HOMO Orbital express the chemical activity and stability of chemical molecules [23]. In addition, the energy of the HOMO orbitals expresses the ionization potential or electron donation (donor), while the LUMO orbitals express the electron affinity or electron acceptance (accepter). The higher value of the HOMO of the molecule tends to donate electrons to a suitable acceptor molecule with low energy and empty molecular orbitals [24].

The total energy, dipole moment, HOMO and LUMO energies, and $\Delta E_{LUMO-HOMO}$ energy gap) of the prepared molecules were calculated in the same way as themolecules were calculated in the same way as the geometric optimization, and their values are shown in dipole moment, HOMO and LUMO energies, and $\Delta E_{LUMO-HOMO}$ energy gap) of the prepared Table 3. From the calculated total energy values, we find that the stability of the compounds follows the following sequence $L3 > L4 > L5 > L1 > L2$, where the compound with the lowest energy is more stable. From looking at the energy difference values between the HOMO and LUMO orbitals shown in Table 3, we find that compound L3 has the lowest value for $\Delta E_{LUMO-HOMO}$, which is 1.271654, which reflects its relative chemical reactivity compared to the other studied compounds, as the lower the ΔE value of the molecule, the more chemically and biologically effective it is. We also note that compound energy gap values, which indicates that these compounds are of low effectiveness. The dipole moment is an electronic measure of the polarity of molecules. When observing the values Theoretically calculated. find that the compounds, L5, L3, L2 has the highest dipole moment. When looking at the shapes of the HOMO and LUMO orbitals of the compounds studied in Table 4, we notice that the HOMO orbitals are mainly centered on sulfur, oxygen and nitrogen, which are the atoms that donate electrons. This confirms that the coordination of these molecules is through these atoms, while the LUMO is centered on the benzene molecule and part of it on the sulfur atom.

2.9 Calculating Mulliken Charge

Atomic and molecular charges can be calculated by calculations performed using computational chemistry using one of the methods developed by Robert S. Mulliken. This method, known as the Mulliken method, is calculated by analyzing the distribution of electronic charges on bonded, non-bonded and antibonded atoms. The Mulliken charge on a single atom can be determined using the lowest level of the basis sets and can be for one negative electron in the orbital or more than two negative electrons in a given orbital. Understanding the nature of atoms and making quantitative predictions about the results of experiments is a great benefit from calculating the Mulliken charge [25][26]. The Mulliken charge was calculated using the same calculation method used for engineering optimization, as the Mulliken charge values express the electron density possessed by the atoms and through these values we can know which atoms have the highest negative potential and the highest basicity, Table 5 and Figure 7 that the two nitrogen atoms have the highest value, which ranges between (-0.428 - -0.613), followed by the oxygen atoms of the carboxyl group (-0.461 - -0.399), then the sulfur atoms (-0.227 - -0.166) in all molecules, so it is expected that the bonding in this type of ligands occurs within the oxygen and nitrogen atoms and sulfur due to the electron density is the highest negative potential.

3 CONCLUSIONS

In this study, a series of benzoyl thiourea derivatives (L1–L5) were successfully synthesized using 4-nitrobenzoyl chloride and 4-methoxybenzoyl chloride with selected aromatic and aliphatic amines. The chemical structures were confirmed by a combination of spectroscopic techniques, including FT-IR, 1H NMR, ^{13}C NMR, and EI-MS, which verified the identity and purity of the synthesized compounds.

After preparing the compounds, identifying them and studying them biologically and theoretically, we conclude that it is easy to prepare carbonyl thiourea compounds after the correctness of the proposed structures has been confirmed using different spectroscopic techniques. If the diagnostic methods prove the correctness of the prepared structures, and the biological study of the prepared compounds

against breast cancer has proven that their biological effectiveness is weak, the computer study has shown that all the prepared compounds were chemically stable based on the values of LUOM and HOMO, and it has also been shown that the electron density is concentrated on the oxygen and sulfur atoms. the analysis identified key donor atoms in each molecule, providing insights into their electronic behavior. The in vitro cytotoxic potential of the synthesized compounds (L1–L5) was assessed against MCF-7 human breast cancer cell lines using the MTT assay. The results revealed that the compounds exhibited low cytotoxic efficacy under the tested conditions.

REFERENCES

- [1] R. Ronchetti, G. Moroni, A. Carotti, A. Gioiello, and E. Camaioni, "Recent advances in urea-and thiourea-containing compounds: focus on innovative approaches in medicinal chemistry and organic synthesis," *RSC Med. Chem.*, vol. 12, no. 7, pp. 1046–1064, 2021.
- [2] N.-Y. Huang, Y.-T. Zheng, D. Chen, Z.-Y. Chen, C.-Z. Huang, and Q. Xu, "Reticular framework materials for photocatalytic organic reactions," *Chem. Soc. Rev.*, 2023.
- [3] U. Zahra, A. Saeed, T.A. Fattah, U. Flörke, and M.F. Erben, "Recent trends in chemistry, structure, and various applications of 1-acyl-3-substituted thioureas: a detailed review," *RSC Adv.*, vol. 12, no. 20, pp. 12710–12745, 2022.
- [4] G. Kirishnamaline, J.D. Magdaline, T. Chithambarathanu, D. Aruldas, and A.R. Anuf, "Theoretical investigation of structure, anticancer activity and molecular docking of thiourea derivatives," *J. Mol. Struct.*, vol. 1225, p. 129118, 2021.
- [5] A.S. Faihan, S.A. Al-Jibori, M.R. Hatshan, and A.S. Al-Janabi, "Antibacterial, spectroscopic and X-ray crystallography of newly prepared heterocyclic thiourea dianion platinum (II) complexes with tertiary phosphine ligands," *Polyhedron*, vol. 212, p. 115602, 2022.
- [6] V. Singh, S. Singh, A. Verma, R.R. Choudhary, and S. Gupta, "Synthesis, characterization and solid state conductivity of nitro-phenol-benzaldehyde urea based ligand and trithiocarbonate," *Mater. Today Proc.*, vol. 51, pp. 496–501, 2022.
- [7] E. Khan, S. Khan, Z. Gul, and M. Muhammad, "Medicinal importance, coordination chemistry with selected metals (Cu, Ag, Au) and chemosensing of thiourea derivatives. A review," *Crit. Rev. Anal. Chem.*, vol. 51, no. 8, pp. 812–834, 2021.
- [8] F.U. Rahman, A.B. Shah, M. Muhammad, F.S. Ataya, and G.E.-S. Batiha, "Antioxidant, antibacterial, enzyme inhibition and fluorescence characteristics of unsymmetrical thiourea derivatives," *Heliyon*, vol. 10, no. 10, 2024.
- [9] Z. Gul, S. Khan, and E. Khan, "Organic molecules containing N, S and O heteroatoms as sensors for the detection of Hg (II) ion; coordination and efficiency toward detection," *Crit. Rev. Anal. Chem.*, vol. 54, no. 6, pp. 1525–1546, 2024.
- [10] A.A. Al-Abbassi, S.F. Kayed, and M.B. Kassim, "Spectral, theoretical, physicochemical and corrosion inhibition studies of ortho-, meta- and para-hydroxyphenyl-benzoylthiourea ligands," *Inorg. Chem. Commun.*, vol. 156, p. 111155, 2023.
- [11] S. Kundu, T.K. Egboluche, and M.A. Hossain, "Urea- and thiourea-based receptors for anion binding," *Acc. Chem. Res.*, vol. 56, no. 11, pp. 1320–1329, 2023.
- [12] M. Muhammad, S. Khan, S.A. Shehzadi, Z. Gul, H.M. Al-Saidi, A.W. Kamran, and F.A. Alhumaydhi, "Recent advances in colorimetric and fluorescent chemosensors based on thiourea derivatives for metallic cations: A review," *Dye. Pigment.*, vol. 205, p. 110477, 2022.
- [13] R.A. Muhammed, B.H. Abdullah, and H.S. Rahman, "Synthesis, cytotoxic, antibacterial, antioxidant activities, DFT, and docking of novel complexes of Palladium (II) containing a thiourea derivative and diphosphines," *J. Mol. Struct.*, vol. 1295, p. 136519, 2024.
- [14] S. Swaminathan, P. Jerome, R.J. Deepak, R. Karvembu, and T.H. Oh, "Platinum group metal (PGM) complexes having acylthiourea ligand system as catalysts or anticancer agents," *Coord. Chem. Rev.*, vol. 503, p. 215620, 2024.
- [15] Y.M. Al-Salim and R.H. Al-Asadi, "Synthesis, anti-breast cancer activity, and molecular docking studies of thiourea benzamide derivatives and their complexes with copper ion," *Trop. J. Nat. Prod. Res.*, vol. 7, no. 6, 2023.
- [16] A.R. Al-Ameertaha and R.H. Al-Asadi, "Synthesis, characterization, and anticancer evaluation of thiourea benzamide derivatives and their Cu (II) and Pt (IV) complexes against PC3 and HepG2 cancer cell lines," *Trop. J. Nat. Prod. Res.*, vol. 8, no. 11, 2024.
- [17] N. Arshad, M. Rafiq, R. Ujan, A. Saeed, S.I. Farooqi, F. Perveen, P.A. Channar, S. Ashraf, Q. Abbas, A. Ahmed, T. Hokelek, M. Kauri, and J.P. Jasinski, "Synthesis, X-ray crystal structure elucidation and Hirshfeld surface analysis of N-((4-(1 H-benzo [d] imidazole-2-yl) phenyl) carbamothioyl) benzamide: Investigations for elastase inhibition, antioxidant and DNA binding potentials for biological applications," *RSC Adv.*, vol. 10, no. 35, pp. 20837–20851, 2020.
- [18] F. Faye, R. Sylla-Gueye, L.E. Thiam, J. Orton, S. Coles, and M. Gaye, "Synthesis, characterization and crystal structure of 1-(2-benzamidophenyl)-3-benzoylthiourea hemihydrate," *Sci. J. Chem.*, vol. 8, no. 6, pp. 131–135, 2020.
- [19] F.A. Saad, "Coordination chemistry of some first row transition metal complexes with multi-dentate ligand (1-benzoyl-3-(4-methylpyridin-2-yl) thiourea), spectral, electrochemical and X-ray single crystal studies," *Int. J. Electrochem. Sci.*, vol. 9, pp. 4761–4775, 2014.

- [20] R.G. Silveira, A.J. Catão, B.N. Cunha, F. Almeida, R.S. Correa, L.F. Diniz, J.C. Tenório, J. Ellena, A.E. Kuznetsov, and A.A. Batista, "Facile synthesis and characterization of symmetric N-[(phenylcarbonyl)carbamothioyl]benzamide thiourea: Experimental and theoretical investigations," *J. Braz. Chem. Soc.*, vol. 29, no. 12, pp. 2502–2513, 2018.
- [21] A.N. Abd Halim and Z. Ngaini, "Synthesis and bacteriostatic activities of bis (thiourea) derivatives with variable chain length," *J. Chem.*, 2016.
- [22] A.R. Al-Ameertaha and R.H. Al-Asadi, "Design, synthesis, characterization, DFT, molecular docking studies and evaluation of biological activity of benzamidethiourea derivatives against HepG2 hepatocellular carcinoma cell lines," *Trop. J. Nat. Prod. Res.*, 2025.
- [23] A.N.A. Fayez, A.F. Ibrahim, and A.A. Saher, "Synthesis, characterization, anticorrosion and biological studies of some new heterocyclic compounds and their complexes," 2020.
- [24] H.M. Qadr and D.M. Mamand, "Molecular structure and density functional theory investigation corrosion inhibitors of some oxadiazoles," *J. Bio Tribo-Corrosion*, vol. 7, no. 4, p. 140, 2021.
- [25] S. Gupta, A.K. Gupta, and B.K. Pandey, "First-principle study on ionic pair dissociation in PEO-PVP-NaClO₄ blend for solid polymer electrolyte," *Polym. Bull.*, vol. 79, no. 7, pp. 4999–5018, 2022.
- [26] Y. Yan, J. Lin, T. Xu, B. Liu, K. Huang, L. Qiao, S. Liu, J. Cao, S.C. Jun, Y. Yamauchi, and J. Qi, "Atomic-level platinum filling into Ni-vacancies of dual-deficient NiO for boosting electrocatalytic hydrogen evolution," *Adv. Energy Mater.*, vol. 12, no. 24, p. 2200434, 2022.